

Single cell electrophysiological alterations under dynamic loading at ultrasonic frequencies

M. Tamayo-Elizalde, C. Kayal, H. Ye, A. Jerusalem*

Department of Engineering Science, University of Oxford

Abstract

The use of ultrasound as a non-invasive means to modulate neuronal electrophysiological signals in experimental *in vivo* and *in vitro* models has recently been gaining momentum. Paradoxically, the intrinsic mechanisms linking high-frequency minute mechanical vibrations to electrophysiological alterations at the cellular scale are yet to be identified in this context. To this end, this work combines patch clamp and nanoindentation to study the action potential alterations induced by direct mechanical vibrations at ultrasonic frequencies of dorsal root ganglion-derived neuronal single cells. The characteristics of the action potentials are studied under oscillatory shear loadings of 25 and 50 nm displacement amplitudes at frequencies ranging from 250 kHz to 1 MHz. Results show significantly narrower action potentials, with faster depolarisations and shorter rising and falling phases when induced after 1 MHz. The faster action potential dynamics appearing once the oscillation is removed points towards a cumulative or lagged effect of mechanical stimulation at ultrasonic frequencies, also observed in ultrasound neuromodulation studies. It is hypothesised here that this action potential modulation arises as a consequence of remarkable membrane properties changes induced above a threshold frequency, situated between 370 kHz and 960 kHz, and possibly related to membrane stiffening and membrane phase state alterations. These observations demonstrate the ability of mechanical cues at the cellular level to modify the neuronal signal and assert the importance of the direct mechanical vibrations induced by ultrasound stimulation protocols in assisting the observed neuromodulatory effects.

Keywords: Neuron mechanics, Action potential, Mechano-electrical coupling, Ultrasound, Dynamic nanoindentation

1. Introduction

While a growing number of ultrasound (US) neuromodulation experiments successfully achieves neuronal activity alterations in a wide variety of animal

*Corresponding author: antoine.jerusalem@eng.ox.ac.uk

and cellular models [1], the underlying mechanisms of action still remain largely
5 unknown. Furthermore, the diversity in animals and more generally models,
as well as in the experimental conditions employed in each case, prevent al-
together an unanimous identification of optimal frequencies and intensities at
which these observations can be triggered. As such, and in spite of some efforts
in this direction [2], a unified convention on how to report the applied sonication
10 magnitudes (pressure, different conventions of time or space averaged intensi-
ties, etc.) is still lacking, further hindering direct comparisons and challenging
repeatability [3]. Whilst this lack of characterisation has not precluded the de-
velopment of the field, a direct understanding of the mechanisms involved is
needed to fully establish US neuromodulation's efficacy and specificity [4].

15 Mechanical interactions have been suggested as the dominating neuromodu-
lating effect during low intensity focused ultrasound (LIFU) sonications [5, 6, 7,
2, 1]. Barring a few exceptions, mechanistic studies of the influence of mechan-
ical waves on neuronal electrophysiology at the cellular scale remain scarce. *In*
vitro studies have characterised the effects of mechanical stimulation in the lim-
20 ited context of touch or pain sensation [8], neuronal outgrowth [9] and traumatic
brain injury [10, 11]. In regards to electrophysiological effects of dynamic me-
chanical stimuli, early experiments with frog and mouse sciatic nerves achieved
brief and fully reversible enhancement as well as suppression of the amplitude
of the compound action potential (AP) by direct pressure pulses applied with
25 transducer-driven glass and single US pulses [12, 13]. Another study combined
microindentation and a high-density multi-electrode array to stimulate mice
retinae at 0.1, 1 and 10 Hz (significantly below ultrasonic frequencies) and 10,
20, 30 and 60 μm indentation depths [14]. The stimulation evoked a plethora of
different responses, with the main one being a prolonged increase in the firing
30 rate lasting for a few seconds, suggesting that the retina perceived the mechan-
ical stimulation as modulation of the visual input. The mechanical response of
smooth muscle cells to LIFU was also studied, and the results showed fluidisa-
tion of the cytoskeleton and acceleration of its remodelling mechanics [5] as a
consequence of US disrupting bonds within cytoskeletal proteins [15]. Recently,
35 oscillating pistons at 60 Hz (again, below typical US range) and atomic force
microscopy were used to stimulate rat cortical neurons treated with synaptic ac-
tivity inhibitors through global shear stress and local indentation, respectively
[16]. These stimulations evoked transient and sustained calcium activity in neu-
rons, which was not fully inhibited by the blockage of mechanosensitive channels
40 (MSCs), but was suppressed by the application of tetrodotoxin and benipidine
(blockers of voltage-gated sodium and calcium channels, respectively). The au-
thors proposed that subtraumatic forces/pressures applied to neurons evoked
neuronal responses *via* nonspecific gating of ion channels, primarily voltage-
gated. Further calcium responses to mechanical stimulation have been reported
45 by several groups. Dorsal root ganglion (DRG) cells seeded with magnetic nan-
odiscs and subjected to weak alternated magnetic fields at 1 or 5 Hz (once again,
below typical US range) demonstrated the ability to trigger calcium influx by
magnetic torque [17]. An increase in intracellular calcium concentration was also
reported in early results of mechanical stimulation of nodose sensory neurons

[18], which was reversibly blocked by gadolinium, a MSC channel blocker that also modifies membrane lipid packing [19]. In two recent studies, continuous 250 kHz and 500 kHz US stimulation of transgenic mouse brain slices induced calcium signalling increases [20], and stimulation of leech ganglia with a 490 kHz and 8 to 20 kPa US transducer reported an accumulative prolonged depolarisation and faster APs [21]. A theoretical model suggested that the selectivity of US excitation of different cortical neuron subtypes, by changing the stimulation pattern, was driven by the response properties of T-type calcium channels [22]. Although many of these effects have been attributed to mechanosensitive responses, the effects of mechanical stimuli on voltage-gated ion channels have also been suggested.

To date, a precise control of the induced neuromodulatory effects remains elusive. Our approach here is to minimise US-induced effects on the surrounding extracellular medium as well as thermal effects, while singling out the mechanical contribution to neuromodulation. In particular, the proposed approach allows for the characterisation of single cell electrophysiological responses to controlled mechanical oscillations at ultrasonic frequencies, while linking them directly to the (stored and dissipated) mechanical energy perturbations. This is particularly relevant as no study has performed intracellular recordings of single neurons under direct mechanical vibrations at varying ultrasonic frequencies, nor quantified the AP characteristics alterations induced by such mechanical stimuli. In this work, a nanoindenter is used to study the influence of dynamic loads at frequencies of up to 1 MHz for two different indentation oscillating amplitudes, 25 and 50 nm, directly applied to single F11 neurons. Significantly narrower action potentials, faster depolarisations, and shorter rising and falling phases are observed after 1 MHz stimulation, pointing towards a cumulative or lagged effect of mechanical stimulation at ultrasonic frequencies. We hypothesise here that this is due to membrane properties changes induced above a threshold frequency situated between 370 kHz and 960 kHz, which might arise from membrane stiffening and membrane phase state alterations. These observations show that direct mechanical oscillations at ultrasonic frequencies applied to single neurons modulate their APs, thus pointing towards direct membrane mechanical vibrations as a potential contributor to neuromodulation. Overall, the proposed methodology and results shed light on the effects of frequency and amplitude of US neuromodulation protocols in the modulated response, and provide valuable insights into the possible mechanisms of action involved.

2. Materials and Methods

2.1. Cell line

F11 cells (ECACC, UK), hybrids between embryonic rat DRG neurons and mouse N18TG-2 neuroblastoma, and commonly used as model sensory neurons [23, 24, 25], were used in these experiments. They present mature neuronal features such as outgrowth of extensive neurites and spontaneous APs [26].

F11s were expanded and differentiated following published protocols [27] included in Supplementary Information. $\sim 5 \times 10^4$ cells were seeded per glass

bottom dish (Willco Wells, Amsterdam, NL) and differentiated for five days
[23] prior to experiments, topping up the media every two days. F11 cells on
their 5th and 6th differentiation day and passages from 18 to 25 were used
for experiments. Isolated cells with contrasted spherical large somas, showing
neurites elongations were studied.

2.2. Combined mechanical stimulation and electrophysiological recording

Fresh pipettes of 2–5 M Ω resistance values measured in the bath solution
were pulled on the day by a micropipette puller (Model P-1000, Sutter Instru-
ments) and back-filled with intracellular solution (see Supplementary Informa-
tion for the intra- and extracellular ion concentrations). The Chiaro nanoin-
denter (Chiaro, Optics11, Amsterdam, NL) was then calibrated for the extra-
cellular medium, and 2 mL of warmed bath solution were added to a glass
bottom dish of F11 differentiated cells, which was placed in the inverted mi-
croscope stage (Nikon eclipse Ti-Nikon Instruments Inc., US) with the air table
on. The probe was left nearby the cell of interest. The pipette was approached,
applying 1–2 kPa positive pressure to prevent pipette tip contamination, and
the cell soma was patched at one edge. Upon contact with the cell membrane,
2 to 5 kPa negative pressure was applied, and released when the seal resistance
reached 200 M Ω . Voltages were recorded with an Axopatch 700B amplifier and
digitised with a Digidata 1550A data acquisition system, using the pCLAMP
10.5 software (Molecular Devices, US). The voltage signal was sampled at 20
kHz and low-pass filtered at 10 kHz. If the gigaseal was not formed within
the first two minutes, cell and pipette were discarded. When a good and sta-
ble seal of >1 G Ω was obtained, the patched membrane was broken by gentle
suction and the cell spontaneous activity was recorded in gap-free zero current
clamp (I0) mode. If the cell showed stable spontaneous activity, sometime aided
by very low (up to 40 pA) induced currents in current clamp mode (IC), the
nanoindenter was manually brought into contact with the cell soma, opposite
the microelectrode, first by 1 and then by 0.25 μ m steps, and left 1–2 μ m above
the cell surface. These small movements did not displace the micropipette,
whose position was continuously monitored through bright-field imaging. Then,
a quasi-static 500 nm compression was imposed and the high frequency shear
experiments were conducted. Nanoindenter and cell membrane voltage signals
were simultaneously recorded with a PicoScope 4262 (Pico Technology, UK),
sampled at 2 kHz.

2.3. High frequency shear loading

Three different shear frequencies (250, 370 and 960 kHz) were studied.
Probes of 0.05 N/m stiffness and 10 μ m spherical tip radius were used. For
all the tests, a 500 nm static compression in indentation-controlled feedback
loop was maintained, and two different oscillating indentation amplitudes were
compared: 25 and 50 nm (see high frequency piezo calibration in Supplementary
Information). The 500 nm static compression was chosen to maximise cortical
membrane contact [28, 29]. The 25 and 50 nm correspond to shear strains <0.3%

in $\sim 20 \mu\text{m}$ diameter cells, thus ensuring that most of the mechanical effects were concentrated on the cortical membrane solely. Separate experiments were conducted for each frequency and oscillation amplitude combination.

140 For each test, the static load was maintained for 400 s. 160 s were recorded before the vibration started, 80 s during loading, and another 160 s after the oscillation was released. These durations were empirically determined so that enough spontaneous APs could be recorded at each stage, for subsequent statistical analyses. Continuous stimulation was chosen, as it was proven to be as
145 effective as or more effective than pulsed stimuli in focused US neuromodulation protocols [30].

The APs of $N=9$ cells loaded in shear 25 and 50 nm at 250, 370, 960 kHz and 260, 380 and 970 kHz, respectively (see Supplementary Information) were analysed before, during and after loading. In all cases, cells preserved their spon-
150 taneous activity, stable V_{res} and morphology after the stimulation, as checked by microscope inspection, and functional neuronal injury was thus *a priori* neglected.

2.4. AP features extraction

For each combination of frequencies and amplitudes, the features of the
155 spontaneous APs of $N=9$ cells in high frequency shear were compared. If a cell showed stable activity a minute after the first indentation, up to three consecutive loading experiments were conducted, randomly choosing the second and third loading frequencies and amplitudes (see Control experiments below).

The following AP features were extracted as explained in Supplementary
160 Information: AP amplitude, AP width, membrane resting voltage V_{res} , AP threshold voltage V_{th} , rising and falling phases, AP firing frequency and maximum value of the first temporal derivative of the membrane potential dV_m/dt . Each averaged AP feature was normalised by dividing it by its counterpart before the dynamic indentation to account for the AP variability arising from the
165 various phenotypes found within F11s [27].

2.5. Control experiments

The order effect was checked for all the frequencies so that, for each frequency, the trend and significance of the normalised AP features from the second and third indentations did not significantly change from those of the first indentation. The inter-cycle analysis of the highest energy protocol, 970 kHz and
170 50 nm amplitude, is given as an example in Supplementary Information, confirming that reproducible responses without significant attenuation were evoked by repeated mechanical stimulation of neurons, and that the analysed features did not significantly change within cycles, at least for up to three indentations.
175 These results point towards the possibility to submit a cell to a series of tests, the results of which can be taken independently from each other. Similar non significant inter-cycle differences in neuronal activity responses were confirmed in previous mechanical stimulation studies [21, 16].

In addition, a sham experiment with no oscillatory load, but only the static
 180 500 nm indentation held for the total 400 s was performed; the analysed invariant
 APs are included in Supplementary Information.

2.6. Statistical analysis

Statistical analyses of the post-processed electrophysiological data were per-
 formed with GraphPad Prism 6. The significance (defined with a threshold
 185 probability of 0.05) of the observed differences between the three experimental
 phases in terms of normalised mean values of the analysed AP features was
 evaluated by conducting a two-way ANOVA test followed by Tukey’s multiple
 comparisons *post-hoc* test to obtain the multiple comparison p-values. The cor-
 responding p values ranges are indicated in figure captions, and the multiplicity
 190 adjusted p values are included in the Results section.

3. Results

A total of N=9 cells were loaded in shear at 25 and 50 nm and 250, 370 and
 960 kHz, while their electrophysiology was monitored through patch clamp,
 see Figure 1. A minimum of n=4 cells were studied per frequency-amplitude
 195 combination. Note that up to three tests were conducted on one single cell if the
 cell showed stable voltage signal and spontaneous spikes after each loading. The
 validity of this approach, *i.e.* the relative independence and reproducibility of
 a series of shear indentation cycles on the same cell was checked by performing
 a control experiment consisting of three repeated stimulations at 970 kHz and
 200 50 nm (the highest energy configuration, thus the most likely to be affected
 by “cascading” effects between cycles) on the same cell, see Figure 2. Results
 showed that the analysed features did not significantly change within cycles,
 see Supplementary Information, thus justifying the study of different loading
 scenarios on a single cell. An example of the AP shapes and dynamics before,
 205 during and after a 970 kHz and 50 nm load is included in Figure 3.

The analysis of the APs before, during and after the loading experiments is
 shown in Figure 4. Normalised amplitudes, resting voltage values and firing fre-
 quencies do not show significant alterations under any of the studied conditions,
 see Figure 4-A, C, H. The highest frequency case (960 kHz) shows significant
 210 differences in normalised AP width, threshold potential V_{th} , rising and falling
 phases and maximum membrane voltage rate dV_m/dt , see Figure 4-B, D, E,
 F, G. The widths of the APs of cells loaded at 960 kHz are significantly nar-
 rower after 25 and 50 nm loading compared to before and during (adjusted
 ****p < 0.0001, see Figure 4-B). For the 25 nm case, cells also show signifi-
 215 cantly hyperpolarised V_{th} values after dynamic loading (adjusted *p = 0.0408
 and *p = 0.0195 with respect to before and during, respectively, see Figure 4-D).
 The depolarising phase after the 50 nm and 960 kHz loading is significantly
 shorter compared to before and during such loading (adjusted ***p = 0.0008,
 **p = 0.0013, see Figure 4-E). The repolarisation phases for both amplitudes
 220 at the maximum frequency are significantly shorter after the shear indenta-
 tion with respect to during (adjusted **p = 0.0038 for 25 nm and **p = 0.0064

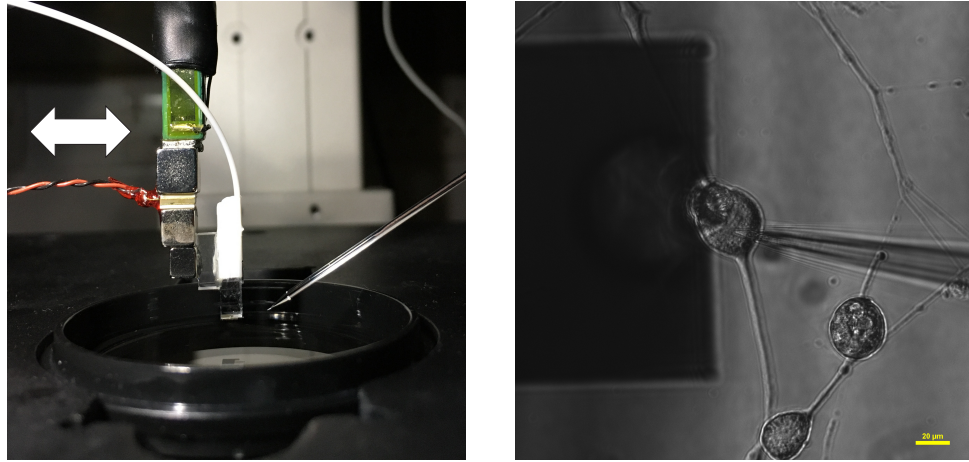


Figure 1: High frequency dynamic module of the nanoindenter in shear configuration (movement direction indicated by white arrow) and patch clamp pipette on the left, with both probes on the same F11 soma on the right. Scale bar is 20 μm .

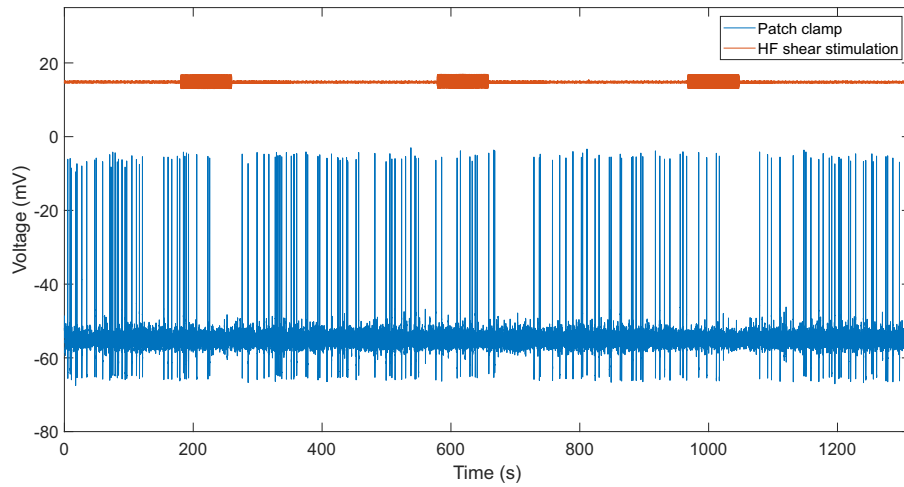


Figure 2: Spontaneous activity of a patched cell indented three times at 970 kHz and 50 nm. The analysed AP features showing no inter-cycle variability are included in Supplementary Information.

for 50 nm, see Figure 4-F). Finally, the maximum values of the time-voltage change ($\max dV_m/dt$) are significantly larger after the 960 kHz oscillations at 25 and 50 nm amplitudes compared to before and during, respectively (adjusted $p=0.408$ and $p^*=0.0195$, see Figure 4-G).

225

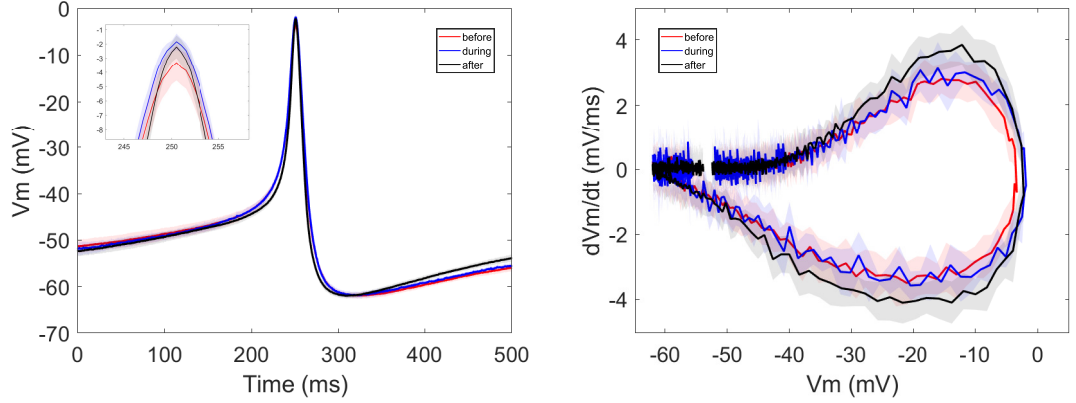


Figure 3: Left: Mean and standard deviation of the APs of a cell loaded at 970 kHz and 50 nm for 80 s, with peaks in the inset. Right: Mean and standard deviation of the phase plots for the same APs; there is non-significant amplitude changes during the loading, but faster AP dynamics appear after the mechanical oscillation (black curve).

4. Discussion

For up to 10 Hz dynamic indentations, both storage and loss moduli of the F11 cell increase with frequency [31]. At higher indentation frequencies, cells thus become stiffer and dissipate more energy. While the cell response is predominantly elastic at these relatively low frequencies, the gap between viscous and elastic effects narrows down with increasing frequencies [31], with suggestions that the former might overtake the latter at around 1 kHz [32] or 60 kHz [29]. Cellular viscoelastic responses at these kHz frequencies are scarce due to technical limitations, but two distinct regimes have been identified and attributed to the fast and the slow dynamics of the cytoskeleton [32], whose individual filamentous components can be excited at high frequencies [29]. The herein induced oscillating amplitudes, comparable to the calculated 30 nm oscillatory displacement induced by LIFU stimulation of smooth muscle cells [5], mainly reach the membrane and membrane cortex, linking the membrane to the underlying cytoskeleton [28, 29]. As these structures determine cellular functionality, the electrophysiological response is anticipated to be affected by the mechanical stimuli [33]. Manifestations of this mechanical-electrophysiological coupling have been observed at different scales. At the organ scale (i.e., brain), stiffness variations with electrical stimulation have been detected [34, 35]. At the cellular scale, altered activity as a result of mechanical [14, 16, 17, 31] and US [21] stimulations has been identified, and membrane stiffness variations at different clamped voltages have been recorded [36]. To date, a precise control of these neuromodulation effects remains however out of reach. Doing so requires a tighter understanding of how the cellular response to a dynamic mechanical stimulus is related to these energy perturbations, both stored and dissipated, whether these are occurring transiently or in a sustained manner, and whether

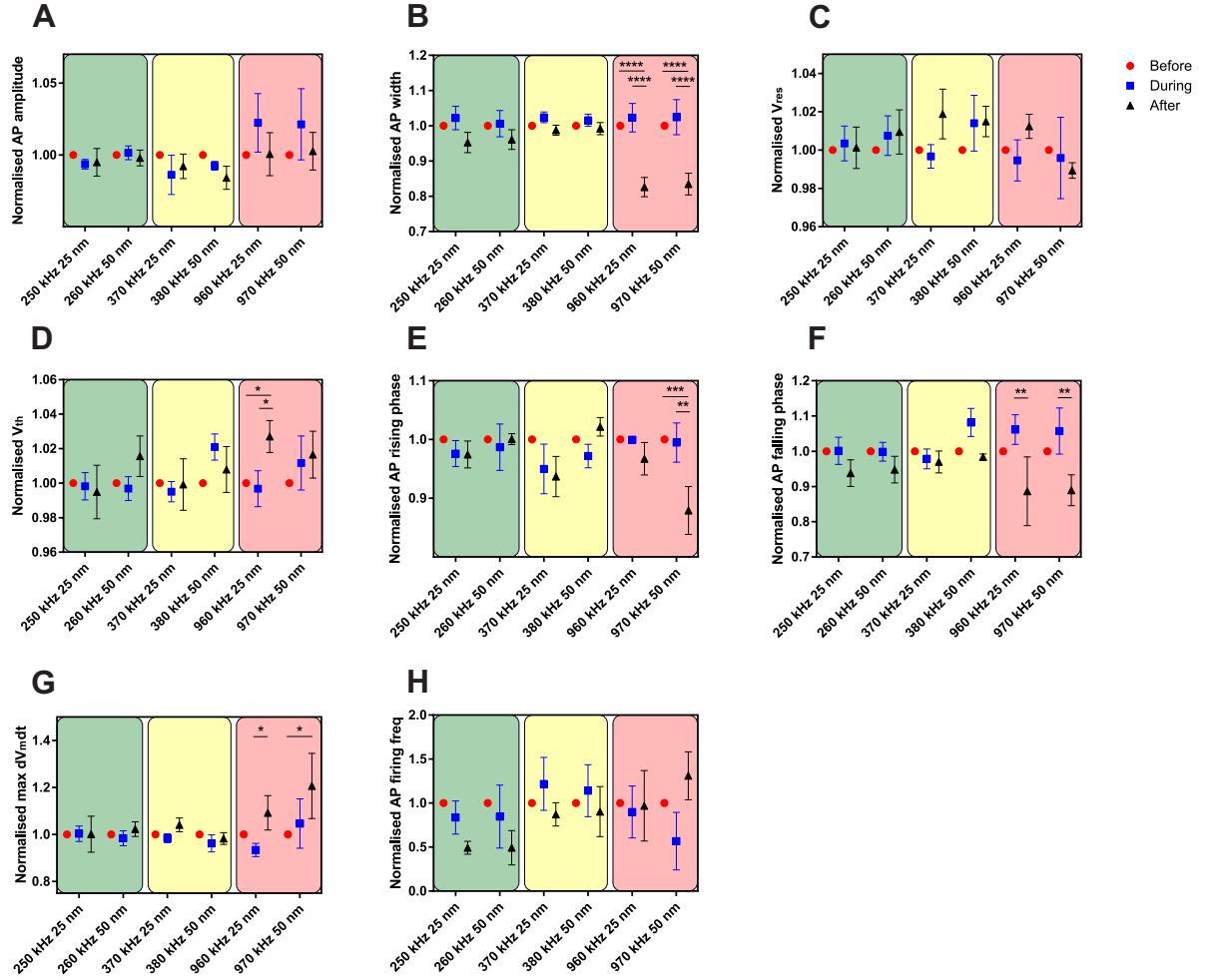


Figure 4: Mean and standard error of the AP features analyses under high frequency shear. A) Normalised AP amplitudes. B) Normalised AP widths. C) Normalised resting membrane voltage values. D) Normalised threshold potential V_{th} . E) Normalised AP rising phases. F) Normalised AP falling phases. G) Normalised maximum membrane voltage rate dV_m/dt values. H) Normalised AP firing frequencies. In B), D), E), F) and G), two-way ANOVA with Tukey's multiple comparisons *post-hoc* tests were performed (* $p < 0.05$; ** $p < 0.01$; *** $p < 0.001$; **** $p < 0.0001$). Note that the during and after data in H) are not statistically significant.

they remain local or become systemic.

Here, electrophysiological changes were recorded through whole cell patch clamping while simultaneously dynamically indenting F11 cells in the US regime, see Figure 4. Significant changes in the analysed AP features appear at the highest studied frequency, 960 kHz. Figure 4 shows faster AP dynamics at vibrations around 1 MHz: significantly narrower (in time) APs after loading (Figure 4-B),

with shorter rising and falling phases after indentation (Figures 4-E and 4-F, respectively). These findings are in agreement with the faster repolarisations observed in mechanically stimulated cells at 60 Hz [16] and 490 kHz [21]. Furthermore, the maximum rate of depolarisation is also significantly larger after 960 kHz shear stimulation at both 25 and 50 nm amplitudes (see Figures 2-right and 4-G), confirming the induced faster voltage dynamics. The threshold voltage is significantly hyperpolarised after the 25 nm amplitude at that same frequency (Figure 4-D). Within each frequency pair, V_{th} values show a hyperpolarisation after larger amplitudes (Figure 4-D), hinting at less depolarising current needed to fire an AP during larger oscillatory indentations. APs modulated at 960 kHz are larger in normalised amplitude during the stimulation (Figures 3 left and 4-A), but smaller during and after 370 kHz loading, although non-significantly. Smaller APs were also found upon 490 kHz stimulation of leech ganglia [21]. Although the firing frequencies decrease overall after the shear stimulation with respect to before, this effect seems to be less pronounced at higher frequencies, and the inverse is actually observed after 960 kHz and 50 nm oscillations (Figure 4-H). A reason for this could be that fast mechanical oscillations propagating through the membrane favour the AP-accompanying mechanical deflections [37, 38] and facilitate cell depolarisation. Increased maximum firing frequencies were observed in rat brain slices stimulated with 43 MHz US [39]. Resting membrane potential (V_{res}) analyses show hyperpolarised cells (Figure 4-C) under 250 and 370 kHz, while cells loaded at 960 kHz show a more depolarising trend, in particular after the largest oscillation amplitudes. Whilst hyperpolarised membrane potentials—as well as narrower APs—were observed under continuous US sonication of rat brain slices at 43 MHz [39] and attributed to the activation of a sustained potassium conductance by US, prolonged and pressure dependent depolarisation was previously reported in cells under 490 kHz US stimulation [21].

Taken altogether, these observations suggest that higher oscillatory shear indentation frequencies promote faster AP dynamics, with a threshold somewhere between 370 and 960 kHz. The effect of quasi-static indentations in compression leads instead to wider and slower APs [31], so there appears to be a threshold frequency above which the induced faster AP modulation effects emerge. In this regime, by shortening its time duration while maintaining its amplitude, the AP requires less electrical energy, thus indicating that a mechanical stimulus of sufficiently high frequency facilitates AP generation and makes the neuronal signal more electrically efficient. From a mechanistic perspective, this could be explained by the increase of stiffness with frequency (and in particular, the cortical membrane), for which the gating mechanisms of the embedded ion channels should be expected to be affected [40, 41, 42, 43, 44], in turn altering the generation and evolution of the AP. Additionally, these fast membrane oscillations could indeed induce membrane area and capacitance changes, found in artificial protein-free lipid membranes stimulated with 1 MHz US [45], that could contribute to the observed effects [31, 46, 47]. From an energetic perspective, the balance between stored energy and dissipated energy (both independently increasing with frequency) is known to swap somewhere in

the kHz regime [32, 29], with a more important proportion of the overall energy being dissipated than stored after this threshold. This notion of “dissipation” could however be understood as an entropy exchange between mechanical features and electrophysiological features, a concept in line with the soliton theory [48, 49]. This could explain why less electrical energy would be required to generate an AP under high frequency stimulation.

Apart from offering a general framework agnostic of the exact mechanism occurring (e.g., capacitance alteration, cavitation, flexoelectricity, etc. [33]), the latter energetic consideration could also help find some ground in explaining the identified threshold in frequency for AP dynamics alteration. Indeed, the AP has been referred to as a propagating membrane phase change [48, 49]. In order for this phase change to occur (from fluid to gel), a local decrease in temperature is needed. In polymer physics, the time-temperature superposition principle establishes that changing a material’s temperature is equivalent to shifting its viscoelastic behaviour by time-dependent means, such as frequency. As such, decreasing the temperature is equivalent to increasing the frequency. This fundamental principle is applicable to brain tissue [50]. Accordingly, lipid membrane phase transitions could be favoured by mechanical vibrations of enough frequency, and these could, in turn, generate, or at the very least, modulate, APs. In practice, the highly inhomogeneous neuronal membrane presents numerous dynamic domains, which are thought to correspond to different membrane phase states [51, 52], and compartmentalise proteins, such as ion channels [53]. The individual and collective responses of these domains are hypothesised here to be altered under direct mechanical stimulation protocols such as the ones presented here, with the corresponding functional alterations observed at the ultrasonic frequencies. **It is finally worth noting that, when a cell is submitted to a pressure wave, shear stresses localise at the boundaries between subcellular components, as opposed to the pressure whose gradient tends to span a larger length scale [54]. The shearing mechanical loading proposed here can thus be expected to induce localised μm (and even nm) intracellular deformations in a similar way as what could be achieved by a mm acoustic pressure wave (i.e., US).**

Most of the altered AP effects only appear after the load is removed, which is more evident at the highest frequency. This points towards a lag or an accumulation of the response, that has already been observed in US studies *in vitro* [21, 55] (attributed to the build-up of intracellular calcium [55, 20]), and *in vivo* (up to 10 min after sonication) [56, 57, 58]. Here, a stress-relaxation mechanical viscous effect coupled to electrophysiology by the membrane mechanical state could explain the observations. Again, energetic considerations whereby the stored energy is released after the end of the stimulation would favour a transfer of energy from mechanics to electrophysiology.

Finally, thermal effects arise naturally when loading viscoelastic solids, and in particular at high frequencies and continuous stimulations such as the ones presented here. However, as the induced shear strains (50 nm over a $\sim 20\ \mu\text{m}$ cell, $\gamma = 0.0025$) and the corresponding maximum shear forces (in excess of 55 pN, as calculated from force-indentation responses) are very small, the generated heat

(which scales with γ^2 [59]) can be expected to quickly diffuse through the surrounding extracellular solution. In this work, the temperature was not directly recorded because a) the feedback system of a stage top incubator routinely used to control the temperature during imaging experiments was found to introduce electrical noise into the patch recorded signal, and b) fitting an extra probe (a thermocouple) within the neuronal soma under study without destabilising or potentially breaking the patch pipette was found to be impractical (see Figure 1-right). No observable major damage was induced in the cells, as monitored *via* microscopy and measurements of stable V_{res} throughout the experiments (ensuring the cell membrane integrity). Furthermore, inter-cycle repeatability during consecutive stimulations was confirmed for the highest energy case (see Supplementary Information), and any heat produced during the loading was expected to dissipate within the 160 s recorded after the oscillation, where most of the significant changes are observed. As such, it is not believed here that thermal effects played a leading role in the observed changes.

5. Conclusions

This work illustrates the capability of the multiphysics setup introduced in Ref. [31] to mechanically load single neurons up to 1 MHz in shear. The proposed methodology provides a quantitative framework to mechanically stimulate neurons at ultrasonic frequencies, while cells are monitored *via* direct microscopy throughout. Results show that direct mechanical vibrations transmitted to the cellular membrane and the underlying membrane cortex modulate the neuronal AP. In particular, frequencies above a threshold situated between ~ 400 kHz and ~ 1 MHz were observed to accelerate AP dynamics, in agreement with other works showing a strengthening of the neuromodulation in the same range [1, 30, 60, 61]. In addition, these results are mostly noted once the oscillation is removed, suggesting a cumulative or lagged effect. These observations are hypothesised here to be related to the stiffening of the membrane and membrane cortex as a result of the mechanical oscillations, thus emphasising the role of the membrane and its mechanical properties on the AP shape and firing process.

Although the membrane mechanical properties alterations induced by these high frequency vibrations might be linked to those induced by US in neuronal tissue, a direct extrapolation of these results to the mechanisms of US neuromodulation needs to account for several discrepancies: a) the applied localised (μm length scale) vibrations *vs.* the more systemic (mm length scale [1, 4]) US neuromodulation, b) the small oscillating amplitudes (50 nm) *vs.* the observed larger quasi-static displacement (18-300 μm induced by 1–5 MPa at 4 MHz in mice sciatic nerves [62]¹) and the similar differences in force magnitude (55 pN *vs.* 873 nN applied to *C. elegans* worm through sonication at 10 MHz, 1 kHz

¹with the caveat that the former corresponds to the dynamic oscillating displacement while the latter corresponds to the net quasi-static displacement arising from the “radiation force”

390 pulse repetition frequency and 50% duty cycle, as predicted with the k-Wave
 toolbox [2]), c) the duration of the stimulus (80 s *vs.* the hundreds of ms of
 pulsed US protocols [63]), and d) only the effects of shear in the specific direction
 of indentation are studied here, while US induces a combination of longitudinal
 and shear waves in multiple directions [64].

395 Future complementary works could be directed to study the influence of in-
 termediate frequencies (especially those between 370 and 960 kHz, aiming at
 finding the threshold frequency for the observed MHz effects) and larger am-
 plitudes, different pulsed protocols, as well as explore the responses when the
 vibrations are sent to axons and dendrites (or even synapses), instead of cell
 400 somas. The activity of neighbouring neurons could also be tracked, in order
 to infer the influence of modulated APs in single cells within a network. Fur-
 thermore, temperature sensitive fluorescent probes or infrared thermography
 methods could be used in future studies to measure potential temperature in-
 crements at high indentation frequencies with minimal invasiveness. Finally,
 405 phase membrane indicators such as Laurdan, a membrane dye that changes flu-
 orescence as a result of alterations in the lipid packing density [65], could be
 used to identify possible membrane phase changes induced by high frequency
 indentations.

On a final note, we also argue here that the many physical processes simul-
 410 taneously at play in US neuromodulation realistically preclude the identifica-
 tion of one unique leading mechanism. Instead, an approach where energetic
 contributions—and thus exchange between physical processes (e.g., mechani-
 cal, thermal, biochemical, electrophysiological)—could hold the key to a more
 systemic and scalable understanding of the intertwined relationship between
 415 US and functional alterations. Such approach clearly requires the design of
 novel experimental methods to capture entropy and enthalpy as the quantities
 of interest, as opposed to what traditional experimental techniques do measure,
 but could, in turn, favour the development of new frameworks focused on the
 transfer of information instead of the information itself.

420 Conflicts of interests

The authors confirm that they have no conflict of interest.

Acknowledgments

The authors acknowledge funding from the EPSRC Healthcare Technologies
 Challenge Award No. EP/N020987/1 and thank Prof. Sonia Contera and Prof.
 425 Ronald Roy for fruitful discussions on cell membrane responses at high frequency
 indentations and US setup calibration process, respectively.

References

- [1] J. Blackmore, S. Shrivastava, J. Sallet, C. R. Butler, R. O. Cleveland,
 Ultrasound Neuromodulation: A Review of Results, Mechanisms and

- 430 Safety, *Ultrasound in Medicine and Biology* 45 (7) (2019) 1509–1536.
doi:10.1016/j.ultrasmedbio.2018.12.015.
- [2] J. Kubanek, P. Shukla, A. Das, S. A. Baccus, M. B. Goodman, Ultrasound
elicits behavioral responses through mechanical effects on neurons and ion
channels in a simple nervous system, *Journal of Neuroscience* 38 (12) (2018)
435 3081–3091. doi:10.1523/JNEUROSCI.1458–17.2018.
- [3] P. D. Edmonds, J. S. Abramowicz, P. L. Carson, E. L. Carstensen, K. L.
Sandstrom, Guidelines for Journal of Ultrasound in Medicine Authors and
Reviewers on Measurement and Reporting of Acoustic Output and Expo-
sure, *Journal of Ultrasound in Medicine* 24 (9) (2005) 1171–1179.
- 440 [4] H. A. S. Kamimura, A. Conti, N. Toschi, E. E. Konofagou, S. A. Lambert,
U. Claude, B. Lyon, Ultrasound Neuromodulation : Mechanisms and the
Potential of Multimodal Stimulation for Neuronal Function Assessment,
Frontiers in Physics 8. doi:10.3389/fphy.2020.00150.
- [5] N. Mizrahi, E. H. Zhou, G. Lenormand, R. Krishnan, D. Weihs, J. P.
445 Butler, D. Weitz, J. J. Fredberg, E. Kimmel, Low intensity ultrasound
perturbs cytoskeleton dynamics, *Soft Matter* 8 (8) (2012) 2438.
- [6] E. Sassaroli, N. Vykhodtseva, Acoustic neuromodulation from a basic sci-
ence prospective, *Journal of Therapeutic Ultrasound* 4 (2016) 17. doi:
10.1186/s40349-016-0061-z.
450 URL <http://www.ncbi.nlm.nih.gov/pmc/articles/PMC4875658/>
- [7] W. Zhou, J. Wang, K. Wang, B. Huang, L. Niu, F. Li, F. Cai, Y. Chen,
X. Liu, X. Zhang, H. Cheng, L. Kang, L. Meng, H. Zheng, Ultrasound
neuro-modulation chip: activation of sensory neurons in *Caenorhabditis*
elegans by surface acoustic waves, *Lab Chip* 17 (10) (2017) 1725–1731.
455 doi:10.1039/C7LC00163K.
URL <http://xlink.rsc.org/?DOI=C7LC00163K>
- [8] A. L. Eastwood, A. Sanzeni, B. C. Petzold, S. J. Park, M. Vergassola, B. L.
Pruitt, M. B. Goodman, Tissue mechanics govern the rapidly adapting and
symmetrical response to touch, *Proceedings of the National Academy of*
460 *Sciences of the United States of America* 113 (17) (2016) E2471. doi:
10.1073/pnas.1604954113.
- [9] Y. Ishibashi, K. Uesugi, K. Morishima, Effect of mechanical stimula-
tion on neurite outgrowth of dorsal root ganglion neurons toward inte-
grative mechanobiologic nerve bridge, SII 2016 - 2016 IEEE/SICE Inter-
national Symposium on System Integration (2017) 797–802doi:10.1109/
465 SII.2016.7844097.
- [10] D. M. Geddes, R. S. Cargill, An in vitro model of neural trauma: De-
vice characterization and calcium response to mechanical stretch, *Journal*
of *Biomechanical Engineering* 123 (3) (2001) 247–255. doi:10.1115/1.
470 1374201.

- [11] D. M. Geddes, R. S. Cargill, M. C. LaPlaca, Mechanical stretch to neurons results in a strain rate and magnitude-dependent increase in plasma membrane permeability., *Journal of neurotrauma* 20 (10) (2003) 1039–1049. doi:10.1089/089771503770195885.
- 475 [12] R. T. Mihran, F. S. Barnes, H. Wachtel, Temporally-specific modification of myelinated axon excitability in vitro following a single ultrasound pulse, *Ultrasound in Medicine and Biology* 16 (3) (1990) 297–309. doi:10.1016/0301-5629(90)90008-Z.
- 480 [13] R. T. Mihran, S. K. Lineaweaver, F. S. Barnes, H. Wachtel, Effects of pulsed acoustic and mechanical stimuli on the excitability of isolated neuronal and cardiac cells, *Applied Occupational and Environmental Hygiene* 11 (4) (1996) 271–274. doi:10.1080/1047322X.1996.10389322.
- 485 [14] M. Marrese, D. Lonardoni, F. Boi, H. van Hoorn, A. Maccione, S. Zordan, D. Iannuzzi, L. Berdondini, Investigating the Effects of Mechanical Stimulation on Retinal Ganglion Cell Spontaneous Spiking Activity, *Frontiers in Neuroscience* 13 (September) (2019) 1–13. doi:10.3389/fnins.2019.01023.
- 490 [15] X. Trepatt, L. Deng, S. S. An, D. Navajas, D. J. Tschumperlin, W. T. Gerthoffer, J. P. Butler, J. J. Fredberg, Universal physical responses to stretch in the living cell, *Nature* 447 (May). doi:10.1038/nature05824.
- 495 [16] B. M. Gaub, K. C. Kasuba, E. Mace, T. Strittmatter, P. R. Laskowski, S. A. Geissler, A. Hierlemann, M. Fussenegger, B. Roska, D. J. Müller, Neurons differentiate magnitude and location of mechanical stimuli, *Proceedings of the National Academy of Sciences of the United States of America* 117 (2) (2020) 848–856. doi:10.1073/pnas.1909933117.
- 500 [17] D. Gregurec, A. W. Senko, A. Chuvilin, P. D. Reddy, A. Sankararaman, D. Rosenfeld, P. H. Chiang, F. Garcia, I. Tafel, G. Varnavides, E. Ciocan, P. Anikeeva, Magnetic Vortex Nanodiscs Enable Remote Magnetomechanical Neural Stimulation, *American Chemical Society Nano* 14 (7) (2020) 8036–8045. doi:10.1021/acsnano.0c00562.
- [18] R. V. Sharma, M. W. Chapleau, G. Hajduczuk, R. E. Wachtel, L. J. Waite, R. C. Bhalla, F. M. Abboud, Mechanical stimulation increases intracellular calcium concentration in nodose sensory neurons, *Neuroscience* 66 (2).
- 505 [19] Y. A. Ermakov, K. Kamaraju, K. Sengupta, S. Sukharev, Gadolinium ions block mechanosensitive channels by altering the packing and lateral pressure of anionic lipids, *Biophysical Journal* 98 (6) (2010) 1018–1027. doi:10.1063/1.3647099.
URL <http://dx.doi.org/10.1016/j.bpj.2009.11.044>
- 510 [20] T. J. Manuel, J. Kusunose, X. Zhan, X. Lv, E. Kang, A. Yang, Z. Xiang, C. F. Caskey, Ultrasound neuromodulation depends on pulse repetition

frequency and can modulate inhibitory effects of TTX, *Scientific Reports* 10 (1) (2020) 1–10. doi:10.1038/s41598-020-72189-y.
 URL <https://doi.org/10.1038/s41598-020-72189-y>

- 515 [21] F. Dedola, F. P. U. Severino, N. Meneghetti, T. Lemaire, A. Cafarelli,
 L. Ricotti, A. Menciasci, A. Cutrone, A. Mazzoni, S. Micera, *Ultrasound
 Stimulations Induce Prolonged Depolarization and Fast Action Potentials
 in Leech Neurons*, *IEEE Open Journal of Engineering in Medicine and Biol-
 ogy* 1 (November 2019) (2020) 23–32. doi:10.1109/ojemb.2019.2963474.
- [22] M. Plaksin, E. Kimmel, S. Shoham, *Cell-Type-Selective Effects of*
 520 *Intramembrane Cavitation as a Unifying Theoretical Framework for*
Ultrasonic Neuromodulation, *eNeuro* 3 (3) (2016) ENEURO.0136–15.2016.
 doi:10.1523/ENEURO.0136–15.2016.
 URL [http://eneuro.sfn.org/cgi/doi/10.1523/ENEURO.0136–15.](http://eneuro.sfn.org/cgi/doi/10.1523/ENEURO.0136–15.2016)
 2016{ }5Cn[http://eneuro.org/content/early/2016/05/30/ENEURO.](http://eneuro.org/content/early/2016/05/30/ENEURO.0136–15.2016.abstract)
 525 [0136–15.2016.abstract](http://eneuro.org/content/early/2016/05/30/ENEURO.0136–15.2016.abstract)
- [23] P. C. Francel, K. Harris, M. Smith, M. C. Fishman, G. Dawson, R. J.
 Miller, *Neurochemical Characteristics of a Novel Dorsal Root Ganglion X
 Neuroblastoma Hybrid Cell Line, F-11*, *Journal of Neurochemistry* 48 (5)
 (1987) 1624–1631.
- 530 [24] S. F. Fan, K. F. Shen, M. A. Scheideler, S. M. Crain, *F11 neuroblastoma ×
 DRG neuron hybrid cells express inhibitory μ - and δ -opioid receptors which
 increase voltage-dependent K⁺ currents upon activation*, *Brain Research*
 590 (1-2) (1992) 329–333.
- [25] J. Prucha, J. Krusek, I. Dittert, V. Sinica, A. Kadkova, V. Vlachova, *Acute*
 535 *exposure to high-induction electromagnetic field affects activity of model*
peripheral sensory neurons, *Journal of Cellular and Molecular Medicine*
 22 (2) (2018) 1355–1362. doi:10.1111/jcmm.13423.
- [26] D. Platika, M. H. Boulos, L. Baizer, M. C. Fishman, *Neuronal traits of*
 540 *clonal cell lines derived by fusion of dorsal root ganglia neurons with neu-
 roblastoma cells.*, *Proceedings of the National Academy of Sciences of the*
United States of America 82 (May) (1985) 3499–3503.
- [27] L. M. Boland, R. Dingledine, *Expression of sensory neuron antigens by a*
dorsal root ganglion cell line, F-11, *Developmental Brain Research* 51 (2)
 (1990) 259–266.
 545 URL <http://www.ncbi.nlm.nih.gov/pubmed/1969775>
- [28] A. G. Clark, K. Dierkes, E. K. Paluch, *Monitoring actin cortex thickness*
in live cells, *Biophysical Journal* 105 (3) (2013) 570–580. doi:10.1016/j.
 bpj.2013.05.057.
 URL <http://dx.doi.org/10.1016/j.bpj.2013.05.057>

- [29] A. Rigato, A. Miyagi, S. Scheuring, F. Rico, High-frequency microrheology reveals cytoskeleton dynamics in living cells, *Nature Physics* 13 (8) (2017) 771–775. doi:10.1038/NPHYS4104.
- [30] R. L. King, J. R. Brown, W. T. Newsome, K. B. Pauly, Effective parameters for ultrasound-induced in vivo neurostimulation, *Ultrasound in Medicine and Biology* 39 (2). arXiv:NIHMS150003, doi:10.1016/j.ultrasmedbio.2012.09.009.
- [31] M. Tamayo-Elizalde, H. Chen, M. Malboubi, H. Ye, A. Jerusalem, Action potential alterations induced by single F11 neuronal cell loading, *Progress in Biophysics and Molecular Biology* doi:10.1016/j.pbiomolbio.2020.12.003.
URL <https://doi.org/10.1016/j.pbiomolbio.2020.12.003>
- [32] L. Deng, X. Trepatt, J. P. Butler, E. Millet, K. G. Morgan, D. A. Weitz, J. J. Fredberg, Fast and slow dynamics of the cytoskeleton, *Nature Materials* 5 (8) (2006) 636–640. doi:10.1038/nmat1685.
URL <http://www.nature.com/doi/10.1038/nmat1685>
- [33] A. Jérusalem, Z. Al-Rekabi, H. Chen, A. Ercole, M. Malboubi, M. Tamayo-Elizalde, L. Verhagen, S. Contera, Electrophysiological-mechanical coupling in the neuronal membrane and its role in ultrasound neuromodulation and general anaesthesia, *Acta Biomaterialia* 97 (2019) 116–140. doi:10.1016/j.actbio.2019.07.041.
URL <https://doi.org/10.1016/j.actbio.2019.07.041>
- [34] S. Patz, D. Fovargue, K. Schregel, N. Nazari, M. Palotai, P. E. Barbone, B. Fabry, A. Hammers, S. Holm, S. Kozerke, D. Nordsletten, R. Sinkus, Imaging localized neuronal activity at fast time scales through biomechanics, *Science Advances* 5 (4). doi:10.1126/sciadv.aav3816.
- [35] L. Qian, Y. Sun, Q. Tong, J. Tian, Z. Ren, H. Zhao, Indentation response in porcine brain under electric fields, *Soft Matter* (2019) 623–632 doi:10.1039/C8SM01272E.
URL <http://xlink.rsc.org/?DOI=C8SM01272E>
- [36] C. Kayal, M. Tamayo-Elizalde, C. Adam, H. Ye, A. Jérusalem, Voltage driven mechanical alterations of neuronal cell membrane, In preparation.
- [37] A. Gonzalez-Perez, L. D. Mosgaard, R. Budvytyte, E. Villagran-Vargas, A. D. Jackson, T. Heimbürg, Solitary electromechanical pulses in lobster neurons, *Biophysical Chemistry* 216 (2016) 51–59. doi:10.1016/j.bpc.2016.06.005.
- [38] A. El Hady, B. B. Machta, Mechanical surface waves accompany action potential propagation, *Nature Communications* 6 (6697) (2015) 1–7.

- [39] M. L. Prieto, K. Firouzi, B. T. Khuri-Yakub, D. V. Madison, M. Maduke, Spike frequency-dependent inhibition and excitation of neural activity by high-frequency ultrasound, *The Journal of general physiology* 152 (11). doi:10.1085/jgp.202012672.
- [40] J. A. Lundbæk, P. Birn, A. J. Hansen, R. Søgaaard, C. Nielsen, J. Girschman, M. J. Bruno, S. E. Tape, J. Egebjerg, D. V. Greathouse, G. L. Mattice, R. E. Koeppe, O. S. Andersen, Regulation of Sodium Channel Function by Bilayer Elasticity: The Importance of Hydrophobic Coupling. Effects of Micelle-forming Amphiphiles and Cholesterol, *Journal of General Physiology* 123 (5) (2004) 599–621. doi:10.1085/jgp.200308996.
- [41] J. A. Lundbæk, P. Birn, S. E. Tape, G. E. Toombes, R. Søgaaard, R. E. Koeppe, S. M. Gruner, A. J. Hansen, O. S. Andersen, Capsaicin regulates voltage-dependent sodium channels by altering lipid bilayer elasticity, *Molecular Pharmacology* 68 (3) (2005) 680–689. doi:10.1124/mol.105.013573.
- [42] D. Oliver, C. C. Lien, M. Soom, T. Baukrowitz, P. Jonas, B. Fakler, Functional Conversion between A-Type and Delayed Rectifier K⁺ Channels by Membrane Lipids, *Science* 304 (5668) (2004) 265–270. doi:10.1126/science.1094113.
- [43] D. Schmidt, R. MacKinnon, Voltage-dependent K⁺ channel gating and voltage sensor toxin sensitivity depend on the mechanical state of the lipid membrane, *Proceedings of the National Academy of Sciences of the United States of America* 105 (49) (2008) 19276–19281. doi:10.1073/pnas.0810187105.
- [44] R. Phillips, T. Ursell, P. Wiggins, P. Sens, Emerging roles for lipids in shaping membrane-protein function, *Nature* 459 (7245) (2009) 379–385.
- [45] M. L. Prieto, O. Oralkan, B. T. Khuri-Yakub, M. C. Maduke, Dynamic Response of Model Lipid Membranes to Ultrasonic Radiation Force, *Public Library of Science ONE* 8 (10). doi:10.1371/journal.pone.0077115.
- [46] M. Plaksin, E. Shapira, E. Kimmel, S. Shoham, Thermal Transients Excite Neurons through Universal Intramembrane Mechanoelectrical Effects, *Physical Review X* 8 (1) (2018) 11043. doi:10.1103/PhysRevX.8.011043. URL <https://doi.org/10.1103/PhysRevX.8.011043>
- [47] M. G. Shapiro, K. Homma, S. Villarreal, C. P. Richter, F. Bezanilla, Infrared light excites cells by changing their electrical capacitance, *Nature Communications* 3 (April 2017) (2012) 736. doi:10.1038/ncomms1742. URL <http://www.nature.com/doifinder/10.1038/ncomms1742>
- [48] T. Heimburg, A. D. Jackson, On soliton propagation in biomembranes and nerves, *Proceedings of the National Academy of Sciences* 102 (28) (2005) 9790–9795.

- [49] T. Heimburg, A. D. Jackson, On the action potential as a propagating density pulse and the role of anesthetics, *Biophysical Reviews and Letters* 2 (1) (2007) 57–78. doi:10.1142/S179304800700043X.
- [50] G. W. M. Peters, J. H. Meulman, A. A. H. J. Sauren, The applicability of the time/temperature superposition principle to brain tissue, *Biorheology* 34 (2) (1997) 127–138. doi:10.1016/S0006-355X(97)00009-7.
- [51] H. Kuge, K. Akahori, K. I. Yagyu, K. Honke, Functional compartmentalization of the plasma membrane of neurons by a unique acyl chain composition of phospholipids, *Journal of Biological Chemistry* 289 (39) (2014) 26783–26793. doi:10.1074/jbc.M114.571075.
- [52] F. A. Heberle, G. W. Feigenson, Phase separation in lipid membranes, *Cold Spring Harbor Perspectives in Biology* 3 (4) (2011) 1–13. doi:10.1101/cshperspect.a004630.
- [53] A. Pristerà, M. D. Baker, K. Okuse, Association between tetrodotoxin resistant channels and lipid rafts regulates sensory neuron excitability, *Public Library of Science ONE* 7 (8). doi:10.1371/journal.pone.0040079.
- [54] J. A., D. M., Continuum modeling of a neuronal cell under blast loading, *Acta Biomaterialia* 8 (9) (2012) 3360–3371. doi:https://doi.org/10.1016/j.actbio.2012.04.039.
URL <https://www.sciencedirect.com/science/article/pii/S174270611200195X>
- [55] S. Yoo, D. R. Mittelstein, R. Hurt, J. Lacroix, M. G. Shapiro, Focused ultrasound excites neurons via mechanosensitive calcium accumulation and ion channel amplification, *bioRxiv* (2020) 1–15.
- [56] R. F. Dallapiazza, K. F. Timbie, S. Holmberg, J. Gatesman, M. B. Lopes, R. J. Price, G. W. Miller, W. J. Elias, Noninvasive neuromodulation and thalamic mapping with low-intensity focused ultrasound, *Journal of Neurosurgery* 128 (3) (2018) 875–884. doi:10.3171/2016.11.JNS16976.
- [57] L. Verhagen, C. Gallea, D. Folloni, C. Constans, D. Jensen, H. Ahnine, L. Roumazelles, M. Santin, B. Ahmed, S. Lehericy, M. Klein-Flugge, K. Krug, R. B. Mars, M. F. S. Rushworth, P. Pouget, J. F. Aubry, J. Sallet, Offline impact of transcranial focused ultrasound on cortical activation in primates, *eLife* 8 (2019) e40541. doi:10.7554/eLife.40541.
- [58] D. Folloni, L. Verhagen, R. B. Mars, E. Fouragnan, C. Constans, J. Aubry, M. Rushworth, J. Sallet, Manipulation of Subcortical and Deep Cortical Activity in the Primate Brain Using Transcranial Focused Ultrasound Stimulation, *Neuron* 101 (6) (2019) 1109–1116.e5. doi:10.1016/j.neuron.2019.01.019.
- [59] N. W. Tschoegl, *The Phenomenological Theory of Linear Viscoelastic Behavior*, Vol. 1, Springer-Verlag Berlin Heidelberg, 1989.

- [60] Y. Tufail, A. Matyushov, N. Baldwin, M. L. Tauchmann, J. Georges, A. Yoshihiro, S. I. H. Tillery, W. J. Tyler, Transcranial Pulsed Ultrasound Stimulates Intact Brain Circuits, *Neuron* 66 (5) (2010) 681–694. doi:10.1016/j.neuron.2010.05.008. URL <http://dx.doi.org/10.1016/j.neuron.2010.05.008>
- [61] W. Legon, A. Rowlands, A. Opitz, T. F. Sato, W. J. Tyler, Pulsed Ultrasound Differentially Stimulates Somatosensory Circuits in Humans as Indicated by EEG and fMRI, *Public Library of Science ONE* 7 (12). doi:10.1371/journal.pone.0051177.
- [62] S. A. Lee, H. A. Kamimura, M. T. Burgess, E. E. Konofagou, Displacement Imaging for Focused Ultrasound Peripheral Nerve Neuromodulation, *IEEE transactions on medical imaging* 39 (11) (2020) 3391–3402. doi:10.1109/TMI.2020.2992498.
- [63] L. Di Biase, E. Falato, V. Di Lazzaro, Transcranial Focused Ultrasound (tFUS) and Transcranial Unfocused Ultrasound (tUS) neuromodulation: From theoretical principles to stimulation practices, *Frontiers in Neurology* 10 (JUN). doi:10.3389/fneur.2019.00549.
- [64] D. P. Darrow, Focused Ultrasound for Neuromodulation, *Neurotherapeutics* (2019) 88–99.
- [65] S. Shrivastava, R. O. Cleveland, M. F. Schneider, On measuring the acoustic state changes in lipid membranes using fluorescent probes, *Soft Matter* 14 (47) (2018) 9702–9712. doi:10.1039/c8sm01635f.